Hardware Design for an Angle of Arrival Positioning System

Marco Gunia*, Adrian Zinke*, Niko Joram* and Frank Ellinger*
*Chair of Circuit Design and Network Theory (CCN)
Technische Universität Dresden, 01062 Dresden
Email: marco.gunia@tu-dresden.de

***Abstract*—Nowadays, there are a variety of different indoor positioning systems employing diverse techniques. Besides inertial navigation, most systems are based on ranging. For instance, techniques utilizing the Received Signal Strength (RSS), phase-difference, time of flight or time of arrival usually convert this information to distances, where trilateration is used to calculate the position. In contrast, approaches utilizing the Angle of Arrival (AoA) are commonly overlooked in literature. Within this paper, we present the hardware design for building such a system and give an outlook towards the algorithms to determine of the AoA. Preliminary measurements show the operability of the system.**

***Keywords*—Localization, Positioning, Angle of Arrival**

I. Introduction

Modern hardware platforms are typically advertised by means of new localization features. For outdoor applications, customers expect an integration of the Global Positioning System (GPS), which is a low-cost readily available solution. For indoor, there exist a multitude of isolated techniques ranging from cheap and inaccurate RSS-based variants with errors up to 30 m [1] to proprietary approaches like Frequency Modulated Continuous Wave- (FMCW) radar, exhibiting errors well below 1 m. Furthermore, there are already commercial off-the-shelf Integrated Circuit (IC). Offering decimetre accuracy, the *Decawave DW1000* enables the setup of an Ultra-WideBand- (UWB) radar [2]. An alternative with comparable accuracy and costs is phase-based ranging by means of the *Atmel AT86RF233* IC [3]. These indoor approaches have in common that the measured quantity is converted to ranges by means of a channel model. Afterwards, the position is obtained with the help of some form of trilateration, e.g. least squares. In contrast to these ranging-based variants, there are techniques employing the angle of incidence, where the final position is determined by triangulation. In hybrid systems, this provides another quantity which can be used to improve the positioning estimate from classical ranging-based techniques.

In this paper, the hardware design for an AoA positioning system is introduced by employing off-the-shelf components, with the overall goal to reduce time to market. Another requirement on the system is to be prepared for hybrid localization in future releases. The rest of this paper is organized as follows. In section II, related research is shortly introduced. This is followed by the general principle in section III. We present the hardware design in section IV. Preliminary results are illustrated in section V. The last section concludes the paper.

II. Related Work

AoA systems can broadly be classified into beam former and subspace-based techniques. Beam former steer and shape the beam, e.g. by utilizing antenna characteristics or by employing digital orientation within multiple antenna designs. In contrast, subspace-based algorithms subdivide the covariance matrix of the received signal into a signal and noise space by singular value decomposition. An orthogonal categorization is the classification into parametric and spectral algorithms. Parametric approaches directly determine the angle of incidence, e.g. by solving equation systems. In contrast, spectral techniques calculate a spectrum, showing power, amplitude or signal strengths as a function of the angle of incidence, where peaks determine the angle estimate [4]. Below, we introduce one variant from each of these 2×2 categories.

The reference signal method, presented in detail in section III, is a parametric beam former. It determines the angle by measuring the phase of the incident signal on every antenna in relation to a local reference. Beneficial is the low complexity, however the signal shape must be known, only one sender can be identified and the method is prone to time-dependent frequency drifts. Bartlett is a classical spectral beam former, where the main lobe of the antenna is digitally moved back and forth to record a spectrum. It has low complexity and no a-priori knowledge about the signal characteristics is necessary. However, the resolution depends on the antenna configuration [5]. ESPRIT [6] is a parametric subspace-based approach consisting of multiple antennas. A prerequisite is a constant distance between adjacent antenna elements, thus ideally the incident signal exhibits the same timely displacement between adjacent antenna elements. ESPRIT firstly determines the covariance matrix and calculates the signal and noise space in a second step. Afterwards, the distance can be calculated directly. MUSIC, which is a spectral subspace-based approach, is similar to ESPRIT in its first steps, but determines a spectrum in its final phase instead [4], [6]. Beneficial is its high resolution, its independence on the shape of the incident signal and the recognition of multiple senders. However, the amount of senders must be known a-priori, the computing complexity is high and there are strong requirements concerning the equivalence in the multiple receiving paths.

III. Determining the angle of arrival

Below, we present the general principle for determining the angle of arrival. Let A be a sending node, transmitting a

https://doi.org/10.24355/dbbs.084-201907151159-0

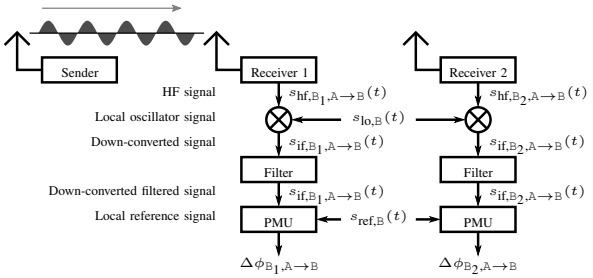

Fig. 1. Receiving path

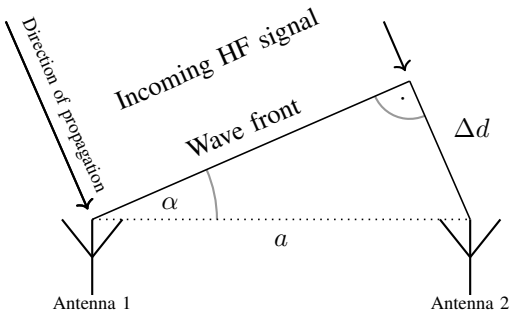

Fig. 2. Wave front of HF signal

sinusoidal signal (index: hf) with frequency $\mathrm{f}_{\mathrm{hf,A}}$

$$s_{\mathrm{hf,A,A\to B}}(t) = \underbrace{A_{\mathrm{hf,A}}(t)}_{:=1} \sin\left(2\pi f_{\mathrm{hf,A}} t + \varphi_{\mathrm{hf,A}}\right) \tag{1}$$

where without loss of generality it is assumed $A_{\mathrm{hf,A}}(t) = 1$. Let B be a two-antenna receiving node, where the antennas are separated by a distance a, as shown in Fig. 2. The above signal received at the first antenna (index: B_1) reads

$$s_{\mathrm{hf,B_1,A\to B}}(t) = \sin\left(2\pi f_{\mathrm{hf,A}}\left[t - \frac{d_1}{c}\right] + \varphi_{\mathrm{hf,A}}\right) \tag{2}$$

Considering Fig. 2, the signal travels an additional distance Δd to the second antenna

$$\Delta d = d\,\sin(\alpha) \tag{3}$$

which is equivalent to an additional propagation time $\Delta d/c$. Thus, we have for the received signal at antenna 2 (index: B_2)

$$s_{\mathrm{hf,B_2,A\to B}}(t) = \sin\left(2\pi f_{\mathrm{hf,A}}\left[t - \frac{d_1}{c} - \frac{\Delta d}{c}\right] + \varphi_{\mathrm{hf,A}}\right) \tag{4}$$

For simplicity we assume that both signals are down-converted by means of the same local oscillator (index: lo)

$$s_{\mathrm{lo,B}}(t) = \sin\left(2\pi f_{\mathrm{lo,B}} t + \varphi_{\mathrm{lo,B}}\right) \tag{5}$$

as illustrated in Fig. 1. Analogous to [3], these down-converted signals (index: if) read

$$\begin{aligned} &s_{\mathrm{if,B_1,A\to B}}(t) \\ &= \sin\left(2\pi f_{\mathrm{if,B}} t - 2\pi f_{\mathrm{hf,A}}\left[\frac{d_1}{c}\right] + \varphi_{\mathrm{hf,A}} - \varphi_{\mathrm{lo,B}} + \frac{\pi}{2}\right) \\ &s_{\mathrm{if,B_2,A\to B}}(t) \\ &= \sin\left(2\pi f_{\mathrm{if,B}} t - 2\pi f_{\mathrm{hf,A}}\left[\frac{d_1}{c} + \frac{\Delta d}{c}\right] + \varphi_{\mathrm{hf,A}} - \varphi_{\mathrm{lo,B}} + \frac{\pi}{2}\right) \end{aligned} \tag{6}$$

where $f_{\mathrm{if,B}} := f_{\mathrm{hf,A}} - f_{\mathrm{lo,B}}$. Afterwards, these signals are compared to a local reference $s_{\mathrm{ref,B}}(t)$ with equal frequency

$$s_{\mathrm{ref,B}}(t) = \sin\Big(2\pi f_{\mathrm{ref,B}} t + \varphi_{\mathrm{ref,B}}\Big) \quad ; \quad f_{\mathrm{ref,B}} := f_{\mathrm{if,B}} \tag{7}$$

to obtain phase differences $\Delta\phi_{\mathrm{B_i,A\to B}}$ to antenna i $(i = 1, 2)$ [7]. Doing so, we have

$$\begin{aligned} \Delta\phi_{\mathrm{B_1,A\to B}} &= -2\pi f_{\mathrm{hf,A}}\left[\frac{d_1}{c}\right] + \varphi_{\mathrm{hf,A}} - \varphi_{\mathrm{lo,B}} + \frac{\pi}{2} - \varphi_{\mathrm{ref,B}} \\ \Delta\phi_{\mathrm{B_2,A\to B}} &= -2\pi f_{\mathrm{hf,A}}\left[\frac{d_1}{c} + \frac{\Delta d}{c}\right] + \varphi_{\mathrm{hf,A}} - \varphi_{\mathrm{lo,B}} + \frac{\pi}{2} - \varphi_{\mathrm{ref,B}} \end{aligned} \tag{8}$$

Subtracting these phase differences, we obtain a formula for the incident angle α

$$\Delta\phi_{\mathrm{B_1,A\to B}} - \Delta\phi_{\mathrm{B_2,A\to B}} = 2\pi f_{\mathrm{hf,A}}\frac{\Delta d}{c} = 2\pi f_{\mathrm{hf,A}}\frac{d\,\sin(\alpha)}{c} \tag{9}$$

where eq. (3) was used. Reordering, we have

$$\sin(\alpha) = \frac{c\left(\Delta\phi_{\mathrm{B_1,A\to B}} - \Delta\phi_{\mathrm{B_2,A\to B}}\right)}{2\pi\ f_{\mathrm{hf,A}}\ d} \tag{10}$$

Above, we assumed that both signals are down-converted by means of the same local oscillator and evaluated with respect to the same reference. It is only mentioned in passing, that both assumptions are not essential and could be discarded in a productive system.

IV. Hardware Design

Below, we present the hardware, where we limit ourselves to the design of the Printed Circuit Board (PCB), which is shown in Fig. 3. On the long back side, there are SMA connectors for four 2.4 GHz antennas, where each is controlled by a single RF transceiver. Here, we employ the *Atmel AT86RF215*. These are placed close to these connectors, where the length of the wires between antenna and transceiver are kept equal for all IC. Moreover, at each transverse side, there is an additional SMA connector for 0.9 GHz communication, respectively. The system is controlled by a *Lattice iCE40HX8K* Field Programmable Gate Array (FPGA), which is responsible for parallel configurating the RF transceiver via the Serial Peripheral Interface (SPI). In turn, the transceiver generate Low Voltage Differential Signaling (LVDS) data at 128 MBit/s, being converted by LVDS converters to single-ended signals. The FPGA either stores the data stream within an 16 MBit SRAM or directly transfers it to a host via Universal Serial Bus (USB) 3.0. The distance between the USB entities and the 2.4 GHz nets are selected as far away as possible to avoid coupling into these high frequency nets. For configuration and debugging, the PCB contains five switches, eight LED and an eight pin General Purpose Input Output (GPIO) header. The FPGA can either be configured via SPI, a separate flash memory or a programming interface. The PCB described so far is a stand-alone solution. However, it can easily be included within our hybrid positioning system [2], [3], by assembling the 100 pin connectors on the front side, which are left empty in Fig. 3. The PCB is supplied by 5 V Direct Current (DC), either from USB or from the 100 pin connectors. This is converted to 3.3 V, 2.5 V, 1.2 V level for the FPGA. These

https://doi.org/10.24355/dbbs.084-201907151159-0

DC-DC converters are also placed far away from the high frequency nets. In the following paragraphs, we present the layout regarding two critical design parameters.

Fig. 3. Printed Circuit Board

A. Antenna distance

For determining the AoA, we employ the MUSIC algorithm [8]. The influence of antenna spacing a on the accuracy is analysed in [9]. It is shown that the error decreases with increasing a. [10] argues that the optimal distance is close to $0.5\,\lambda$ and that ambiguities arise for $a > 0.6\,\lambda$. Hence, a should fulfil $0.5\,\lambda \leq a \leq 0.6\,\lambda$. In this work, we select $a := 0.5\,\lambda$. [11] recommends dimensioning the antenna distance for the highest possible frequency, which is 2483.5 MHz for the AT86RF215. In doing so, we have $a = 0.5\,\lambda = 0.5\,{}^{\mathrm{c}}\!/_{\mathrm{f}} = 6.04\,\mathrm{cm}$.

B. Clock generation

The transceivers operate with 26 MHz clock. For determining the AoA, the phase relations of these IC are required. To alleviate frequency drifts between the transceiver, these are connected to the same clock. We used a voltage controlled temperature compensated crystal oscillator, which is placed in the centre of the transceiver. We carefully designed the distances between crystal and all transceiver to be almost equally long. In doing so, the overall clock net length must be minimized to reduce capacitive load to obtain a pure clock.

V. Experiments

In Fig. 4b we present the first preliminary results for a $17\,\mathrm{m} \times 12\,\mathrm{m}$ university hall, shown in Fig. 4. The hall contains pillars, stairs and metallic handrails in the line of sight, hence multi-path is supposed to happen. The receiver is held at a constant position, indicated by the diamond. In contrast, the sender is placed at 64 different positions, characterized by the circles. A very coarse metric is used, where the blue colour indicates differences below $10°$ between the true and measured incident angle. All other measurement points are coloured red. As can be seen, there are many blue points close to the receiver. In contrast, for positions where the signals travel through the metallic handrails, the measurements are worse. Nevertheless, it can be seen that the system is operable.

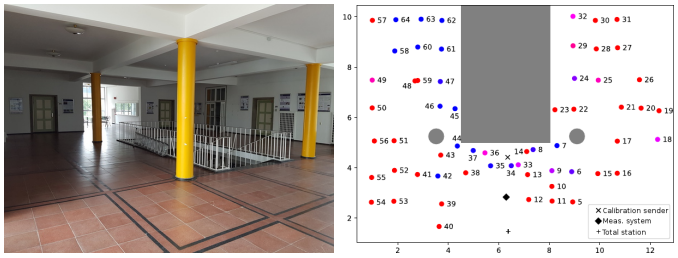

(a) Outline (b) Measurements

Fig. 4. Experiment in university hall

VI. Summary and Outlook

This paper presented the hardware design for an AoA-based positioning system. Besides introducing the general principle together with related work, special emphasis is put on the selection and collaboration of the hardware components for the embedded system. The core is a FPGA, on the one hand being responsible for controlling four RF IC. On the other hand, it sends the measurement data via an USB 3.0 to a host PC, where the angle is calculated by means of a Python script. Finally, the first measurements are presented showing good results in sophisticated multi-path environments.

Acknowledgment

The research leading to these results has received funding from the European Communitys Seventh Framework Programme (FP7/2007-2013) under grant agreement ICT-FP7-611526 (MAGELLAN).

References

[1] H. Liu, H. Darabi, P. Banerjee, and J. Liu, "Survey of wireless indoor positioning techniques and systems," *IEEE Transactions on Systems, Man, and Cybernetics, Part C (Applications and Reviews)*, vol. 37, no. 6, pp. 1067–1080, Nov. 2007, ISSN: 1094-6977. DOI: 10.1109/TSMCC.2007.905750.

[2] M. Gunia, F. Protze, N. Joram, and F. Ellinger, "Setting up an ultra-wideband positioning system using off-the-shelf components," in *2016 13th Workshop on Positioning, Navigation and Communications (WPNC)*, Oct. 2016, pp. 1–6. DOI: 10.1109/WPNC.2016.7822860.

[3] M. Gunia, A. Zinke, N. Joram, and F. Ellinger, "Setting up a phase-based positioning system using off-the-shelf components," in *Proc. 14th Work. Positioning, Navig. Commun. (WPNC'17)*, Bremen, Germany: IEEE, 2017, pp. 1–6. DOI: 10.1109/WPNC.2017.8250065.

[4] S. Ejaz and A. Shafiq, "Comparison of spectral and subspace algorithms for fm source estimation," *Progress in Electromagnetics Research C*, vol. 14, pp. 11–21, Jan. 2010. DOI: 10.2528/PIERC10042705.

[5] C. M. Reustle, "Konzeptionierung, erforschung und erprobung eines 24ghz sekundärradar tachymeters zur präzisen messung der ausladung eines mobilkranes," pp. 1–193, 2018. DOI: urn:nbn:de:bvb:29-opus4-102718.

[6] R. Roy and T. Kailath, "Esprit-estimation of signal parameters via rotational invariance techniques," *IEEE Transactions on Acoustics, Speech, and Signal Processing*, vol. 37, no. 7, pp. 984–995, Jul. 1989, ISSN: 0096-3518. DOI: 10.1109/29.32276.

[7] M. Pelka, C. Bollmeyer, and H. Hellbrück, "Accurate radio distance estimation by phase measurements with multiple frequencies," in *2014 International Conference on Indoor Positioning and Indoor Navigation (IPIN)*, Oct. 2014, pp. 142–151. DOI: 10.1109/IPIN.2014.7275478.

[8] R. Schmidt, "Multiple emitter location and signal parameter estimation," *IEEE Transactions on Antennas and Propagation*, vol. 34, no. 3, pp. 276–280, Mar. 1986, ISSN: 0018-926X. DOI: 10.1109/TAP.1986.1143830.

[9] L. Huang, H. Chen, Y. Chen, and H. Xin, "Research of doa estimation based on music algorithm," Jan. 2016. DOI: 10.2991/mmebc-16.2016.432.

[10] M. Mohanna, M. L. Rabeh, E. M. Zieur, and S. Hekala, "Optimization of music algorithm for angle of arrival estimation in wireless communications," *NRIAG Journal of Astronomy and Geophysics*, vol. 2, no. 1, pp. 116–124, 2013. DOI: 10.1016/j.nrjag.2013.06.014.

[11] H. Tang, "Doa estimation based on music algorithm," *Linné-Universität*, 2019.